

Article

Influence of Dielectric Barrier Discharge Plasma Treatment on Corn Starch Properties

Mayara L. Goiana  and Fabiano A. N. Fernandes * 

Departamento de Engenharia Química, Universidade Federal do Ceará, Campus do Pici, Fortaleza 60440-900, CE, Brazil; mayara_goiana@hotmail.com

* Correspondence: fabiano@ufc.br

Abstract: This study evaluated the effects of dielectric barrier discharge (DBD) plasma technology on some physicochemical and structural properties of corn starch. Amylose content, solubility, water absorption index, turbidity, structural relationships, and surface morphology were measured at 100, 200, and 300 Hz excitation frequencies and at 10 and 20 min exposure times. The plasma treatment at 200 Hz and 20 min promoted the most significant modifications in amylose content, solubility, the water absorption index, and surface morphology. Turbidity did not change significantly. The surface of the granule became smoother with the presence of pores. Slight changes were observed in the ordered structure of starch. Plasma changed several physicochemical properties, significantly decreasing the amylose to amylopectin ratio. Plasma treatment at 200 Hz is recommended to increase the amylopectin content in starches.

Keywords: corn starch; amylose; amylopectin; cold plasma



Citation: Goiana, M.L.; Fernandes, F.A.N. Influence of Dielectric Barrier Discharge Plasma Treatment on Corn Starch Properties. *Processes* **2023**, *11*, 1966. <https://doi.org/10.3390/pr11071966>

Academic Editor: Jean-Louis Lanoiselle

Received: 22 May 2023

Revised: 13 June 2023

Accepted: 20 June 2023

Published: 29 June 2023



Copyright: © 2023 by the authors. Licensee MDPI, Basel, Switzerland. This article is an open access article distributed under the terms and conditions of the Creative Commons Attribution (CC BY) license (<https://creativecommons.org/licenses/by/4.0/>).

1. Introduction

Starch is a complex carbohydrate that plays a significant role in the food industry due to its several functional properties, which make it a versatile ingredient in food formulation and manufacturing. Starch is the plant's primary energy reserve found in its tubers, roots, fruits, and seeds. Its structure consists of amylose and amylopectin molecules, with linear and branched chains, respectively. This carbohydrate is widely used in many industrial applications such as food, pharmaceuticals, papermaking, and textiles.

In the food industry, starch is applied as a thickening and stabilizing agent, gelling and binding agent, texture and mouthfeel enhancer, protective coating for shelf-life extension, calorie reduction agent in substitution to fats, and for other applications [1,2].

Native starch has limited uses in the food industry because it is unstable under temperature changes, highly non-reactive, insoluble, and retrogrades easily [3]. To improve their functionality, native starches can be modified through physical, chemical, or enzymatic processes. Physical modifications of starch include retrogradation, extrusion, pre-gelatinization, and particle size reduction [4,5]. Retrogradation produces resistant starches that provide good health benefits. Extrusion improves the solubility, viscosity, and stability of starches. Pre-gelatinization produces rapidly dissolving starch granules. Particle size reduction enhances starch's solubility, dispersibility, and thickening properties. The enzymatic modification of starch includes hydrolysis, isomerization, cross-linking, and depolymerization. Most of the enzymatic processes for starch modification produce lower-molecular-mass compounds, such as oligosaccharides, dextrins, maltose, glucose, and fructose, with applications in syrups, sweeteners, and beverages. Enzymatic cross-linking involves the formation of bonds between starch and amino acids, resulting in modified starches with better stability, texture, and heat resistance [6,7].

Chemical modifications of starch can lead to the improvement of starches' properties and can also enable the development of innovative and functional starches. Chemical

changes in starches include etherification, esterification, cross-linking, oxidation, and acidification [8,9]. Etherification and acidification improve solubility, stability, and thickening properties. Esterification and chemical cross-linking improve heat, acid, and shear resistance. Oxidation improves water-holding capacity, stability, and film-forming properties.

Plasma technology is considered one of the new green technologies due to the reduction in chemical waste attained through its application. Plasma is the fourth state of matter and comprises free radicals, neutral particles, electrons, photons, and ions. It can be generated from ionizing gases through electric or radiofrequency fields [10,11]. Dielectric barrier discharge (DBD) plasma technology operates at low energy levels, ambient pressure, and ambient temperature, providing the fast, economical, efficient, and environmentally friendly physical modification of several organic and inorganic materials [12]. Plasma generated in atmospheric air produces several reactive oxygen and nitrogen species (ROS and RNS) that can react with many organic and inorganic materials. Thus, plasma could be suitable for starch modification since ROS and RNS can lead to hydrolysis, hydrogenation, etherification, cross-linking, oxidation, isomerization, depolymerization, and acidification [13,14].

Cold plasma technologies have been studied to modify starch's physicochemical, thermal, and crystalline properties [15–18]. DBD treatment can alter starch's structure and physicochemical properties without destroying its granules' integrity [12]. Studies with quinoa, rice, sorghum, and wheat starch reduced amylopectin content while increasing the water solubility index, water absorption index, paste viscosities, and digestibility. Such improvements expand its use in food industries, especially as a thickening agent [19,20].

The goals for starch modification depend on its application. Improving its water-holding capacity, heat resistance, and binding properties, and minimizing syneresis is interesting for direct food preparation applications. For applications in edible films, it is interesting to increase its hydrophobicity and amylopectin content and to modify its surface [21]. The reactive species generated by plasma application and, therefore, the reactions induced by plasma depend on the different types of equipment, excitation frequency, processing time, and types of gas that are applied [10]. As such, the proper setup of operating conditions is essential for plasma-induced modifications of starches.

This work has evaluated the effects of dielectric barrier discharge plasma treatment on corn starch's morphological structure and physical–chemical properties when subjected to different plasma generation frequencies and processing times.

2. Material and Methods

2.1. Materials

Commercial corn starch (Maizena brand, Garanhuns, Brazil) was used in this work. An amylose standard was purchased from Merck (Rahway, NJ, USA).

2.2. Plasma Treatment

Corn starch samples were treated with cold plasma using dielectric barrier discharge plasma equipment comprising an energy source (Inergiae model PLS0130, Florianópolis, Brazil) and a treatment chamber. The chamber comprised two 8 cm diameter aluminum electrodes and two 2 mm acrylic plates acting as dielectric barriers. A scheme of the equipment can be found in Fernandes et al. [22].

Petri dishes containing 15 g of starch were placed at the center with the electrodes within the 1.5 cm gap between the dielectric barriers. Plasma was generated at 20 kV (maximum voltage reached with the equipment), at excitation frequencies of 100, 200, and 300 Hz, for 10 and 20 min. The experimental design was based on previous studies of our group that indicated that this range is optimal for inducing chemical and morphological changes in starches. Higher excitation frequencies resulted in insignificant changes to starch [14,19,23].

The samples were stored in sealed aluminum-coated polyethylene/polyethylene terephthalate (PE/PET) bags until analysis. All experiments were carried out in triplicate.

2.3. Starch Characterization

2.3.1. Amylose

The amylose content was determined based on the colorimetric measurement of starch iodine complexes, following the method described by Hu et al. (2016) [24]. The starch sample (0.1 g) was weighed and suspended in 10 mL of NaOH (1 mol/L). The suspension was heated (70 °C) for 15 min in a water bath. After cooling to room temperature, 5 mL of the solubilized starch solution was removed and mixed with 46 mL of water, 1 mL of acetic acid (1 mol/L), and 2 mL of iodine solution (0.2 g I₂ and 2 g KI in 100 mL of water). After staining for 10 min, the absorbance of the solution was read at 620 nm using a UV-vis spectrophotometer (Thermo Scientific model Evolution 201, Waltham, MA, USA). The same solution without adding the solubilized starch solution served as a blank. Acrylic cuvettes were used. The amylose content in the starch sample was determined using a calibration curve built using pure amylose.

2.3.2. Solubility and Water Absorption Index (WAI)

Sample suspensions containing 1% of starch (*w/w*) were stirred at room temperature (25 °C) for 30 min and then centrifuged at 10,000 rpm for 15 min. The supernatant and the residue were poured onto Petri dishes and dried in a drying oven (Tecnal model TE-394/2-MP, Piracicaba, Brazil).

The cold water solubility (*S*%) of the samples was calculated by dividing the weight of the dried supernatant (*W_s*) by the initial starch weight (*W_i*) (Equation (1)) following the method described by Fang et al. (2021) [25].

$$S(\%) = \frac{W_s}{W_i} 100 \quad (1)$$

The water absorption index (*WAI*) of the samples was calculated by dividing the weight of the dried residue (*W_r*) by the initial starch weight (*W_i*) (Equation (2)).

$$WAI(\%) = \frac{W_r}{W_i} 100 \quad (2)$$

2.3.3. Turbidity

The turbidity measurement was performed according to the method described by Chen et al. (2020) [26], with modifications. A 2% (*w/w*) aqueous suspension of corn starch was heated (100 °C) for 1 h and stirred in 5 min intervals. After cooling to room temperature (25 °C), the turbidity was determined by measuring the sample absorbance at 640 nm using a UV-vis spectrophotometer (Thermo Scientific model Evolution 201, China). Water served as blank. Acrylic cuvettes were used.

2.3.4. Chemical Groups and Molecular Structure

The molecular structures of plasma-treated and untreated corn starch samples were analyzed via Fourier transform infrared spectroscopy (FTIR). Analysis was performed using Cary 630 FTIR (Agilent, Santa Clara, CA, USA) equipped with an accessory for ATR measurements. The spectra were collected in the region between 4000 and 400 cm⁻¹. The absorbances in the 995 cm⁻¹ and 1022 cm⁻¹ bands were used to calculate the short-range ordered structure or crystalline/amorphous ratio (*CAR*), which was determined using Equation (3), as proposed by Warren et al. (2016) [27].

$$CAR = \frac{Abs(995 \text{ cm}^{-1})}{Abs(1022 \text{ cm}^{-1})} \quad (3)$$

2.3.5. Morphology

Scanning electron microscopy (SEM) was used to analyze the morphology of the plasma-treated and untreated corn starch samples. Starch samples were mounted on stubs

and metalized with a thin layer (20 nm) of gold using a Quorum QT150ES metallizer. The samples were analyzed using a Quanta 450 FEG-FEI scanning electron microscope with an accelerating voltage of 20 kV.

2.4. Starch Flowability

Starch powder flow was assessed by measuring its consolidation stress, unconfined yield stress, bulk density, and wall friction angles [28]. These measurements were carried out using Powder Flow Tester (PFT, Brookfield Engineering Labs, Essex, UK). Starch (25 g) was placed in circular stainless steel trays and subjected to stresses from 0 to 13.5 kPa to the surface of the starch powder.

2.5. Statistical Analysis

Statistical analysis was performed using analysis of variance (one-way ANOVA) through the Statistica[®] software version 7. Tukey's test was applied at a 95% confidence level to detect significant differences between means.

3. Results and Discussion

3.1. Amylose

Amylose content is an important parameter that determines many properties and applications of starch. The amylose and amylopectin content observed in corn starch and plasma-treated corn starch is presented in Table 1.

Table 1. Amylose and amylopectin content in plasma-treated and untreated corn starch *.

Plasma Generation Frequency	Processing Time	Amylose Content	Amylopectin Content
(Hz)	(min)	(%)	(%)
0	0	24.2 ± 0.3 ^a	75.8 ± 0.3 ^a
100	10	21.6 ± 0.4 ^b	78.4 ± 0.4 ^b
100	20	23.7 ± 0.9 ^{ac}	76.3 ± 0.9 ^c
200	10	22.1 ± 1.2 ^c	77.9 ± 1.2 ^b
200	20	20.8 ± 0.9 ^{bc}	79.2 ± 0.9 ^d
300	10	22.4 ± 0.4 ^c	77.6 ± 0.4 ^b
300	20	23.7 ± 0.4 ^{ac}	76.3 ± 0.4 ^c

* Values in the same column not followed by a common letter are significantly different ($p < 0.05$).

The control sample (untreated corn starch) presented 24.2% of amylose. Plasma treatment reduced the amylose content in corn starch. The highest reduction in amylose content (14%) was observed when it was treated at 200 Hz for 20 min. Plasma tends to depolymerize linear chains of carbohydrate polymers [29,30], producing shorter carbohydrate chains and carbohydrate radicals. At the same time, the free radicals generated in the plasma react with amylose creating internal radicals, which polymerize, producing amylopectin.

All applied operating conditions increased the amylopectin content. The conversion of amylose into amylopectin was higher at 200 Hz, which increased with the processing time. Longer processing times (>20 min) were not tested in this work because previous studies from our group indicated that no changes were obtained after 30 min of plasma treatment. The treatments at 100 and 300 Hz showed an increase in amylopectin content, but after 10 min of treatment, the amylose content tended to increase due to the depolymerization of amylopectin branches.

An increase in amylopectin content has shown to be a regular trend in DBD plasma-treated starches since similar results have been reported for aria [19] and banana starch [23]. Such a trend may be related to the higher concentration of hydroxyl radicals at 200 Hz, which may abstract hydrogens from the starch molecule forming a free radical in the starch and water. The free radical reacts with other starch radicals or depolymerized fragments, generating the branches that characterize the amylopectin molecule. The results differ

from those of microwave-generated plasma, where an increase in amylose content was observed [3]. Thus, the influence of plasma treatment on amylose is also related to the type of plasma technology used in starch processing.

Starches with lower amylose contents and, consequently, higher amylopectin contents influence several starch properties. In general, a higher amylopectin content improves the digestibility of starch since digestive enzymes facilitate access to glucose units in branched starches; it enhances the gelation of starch, leading to practical applications in the food industry and it improves the texture of foods containing starch due to better chewiness, firmness, and overall mouthfeel.

3.2. Solubility and Water Absorbance Index

When starch comes into contact with water, the granules swell slightly due to the diffusion and absorption of water in amorphous regions, which are formed by the interactions of the amylose and amylopectin chains. The relationship between the molecular structure of starch and its behavior in terms of some physicochemical properties suggests that several structural characteristics, such as amylose content, the distribution of amylopectin chain length, and the degree of crystallinity in the granule, could be closely related to the events associated with gelatinization and retrogradation [31].

Table 2 presents data on starch solubility, the water absorbance index, and the degree of turbidity. Starch solubility decreased after plasma treatment under all conditions tested. Decreases higher than 8.5% were observed for starch subjected to plasma treatment at 200 and 300 Hz. Some authors have generically explained this effect as one that is caused by molecular degradation and the oxidation of starch [12]; however, the decrease in solubility is related to the increase in amylopectin during plasma treatment. Similar changes were reported for corn starch [14] and banana starch [23]. However, increases in starch solubility were reported by Sun et al. (2022) [3] using microwave-generated plasma and by Thirumdas et al. (2017) [32] using DBD air plasma.

Table 2. Solubility, water absorption index, and degree of turbidity of starch subjected to DBD plasma *.

Excitation Frequency (Hz)	Processing Time (min)	Solubility (%)	Water Absorption Index (%)	Turbidity
0 (Control)		90.6 ± 0.63 ^a	1.97 ± 0.05 ^a	1.73 ± 0.03 ^a
100	10	83.8 ± 0.60 ^b	1.98 ± 0.11 ^a	1.73 ± 0.01 ^a
100	20	83.7 ± 0.84 ^b	1.97 ± 0.04 ^a	1.78 ± 0.02 ^{ab}
200	10	82.6 ± 1.38 ^{ab}	2.07 ± 0.47 ^{ab}	1.77 ± 0.02 ^{ab}
200	20	84.0 ± 1.17 ^b	2.07 ± 0.16 ^{ab}	1.78 ± 0.02 ^{ab}
300	10	83.3 ± 1.10 ^{ab}	2.10 ± 0.10 ^b	1.77 ± 0.02 ^{ab}
300	20	82.7 ± 0.79 ^{ab}	2.18 ± 0.08 ^b	1.81 ± 0.02 ^b

* Values are the mean of four measurements ± standard deviation; values in the same column not followed by a common letter are significantly different ($p < 0.05$).

Starch water absorption slightly increased in relation to that of the control sample for excitation frequencies between 200 and 300 Hz. The increased hydrophilicity of corn starch treated with DBD plasma was due to the increased hydroxyl content, as evidenced by the FTIR analysis (Figure 1 and Table 3). This result is consistent with that of Yan et al. (2020) [33] and Guo et al. (2022) [12] for DBD-modified banana and corn starch, respectively. The increase in the water absorption index is positive for several food applications because it results in gels with higher viscosity and firmness and helps retain moisture in food products.

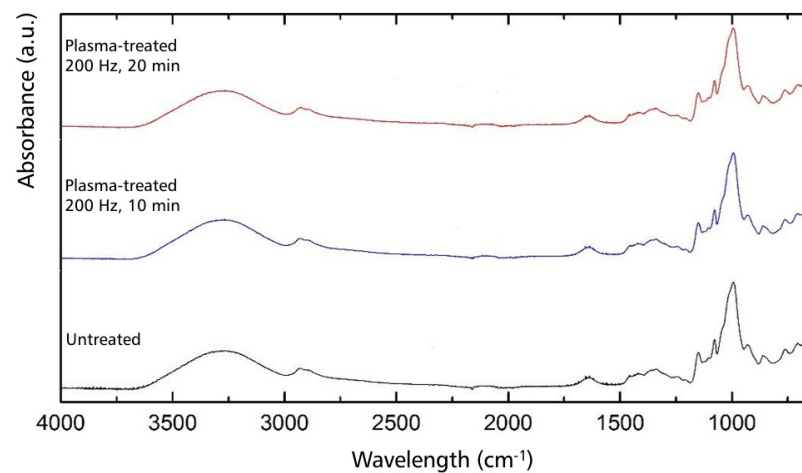


Figure 1. FTIR spectra of corn starch treated with DBD plasma for the control sample and samples treated at 200 Hz.

Table 3. The absorbance of the main FTIR bands of starch.

Freq. (Hz)	Time (min)	Absorbance (cm ⁻¹)										
		2900	1337	1150	1102	1078	1045	1022	995	962	762	703
Control	0	0.085	0.084	0.166	0.140	0.232	0.280	0.402	0.514	0.242	0.180	0.209
	100	0.086	0.084	0.166	0.141	0.230	0.271	0.396	0.500	0.239	0.179	0.206
	100	0.087	0.086	0.170	0.144	0.236	0.284	0.407	0.519	0.246	0.184	0.212
	200	0.098	0.097	0.191	0.161	0.265	0.318	0.459	0.594	0.279	0.208	0.240
	200	0.091	0.089	0.176	0.149	0.244	0.293	0.422	0.537	0.257	0.190	0.217
	300	0.089	0.087	0.172	0.144	0.238	0.286	0.411	0.525	0.246	0.188	0.216
	300	0.085	0.083	0.167	0.141	0.233	0.282	0.405	0.517	0.244	0.180	0.207

3.3. Turbidity

The turbidity remained stable after plasma treatment (Table 2). Only the sample treated at 300 Hz for 20 min differed significantly from the control sample, with an increase of 5%, probably due to the increase in the molecular weight of starch [26]. Thus, plasma had no significant effect on the starch solution's turbidity.

3.4. Molecular Structure

The FTIR spectra for all tested samples showed few differences between themselves and the control, with slight changes caused to starch treated at 200 Hz (Figure 1). Infrared spectroscopy is sensitive to changes in starch's molecular structure, such as helical chain conformation, crystallinity, the retrogradation phenomenon, and water content [34].

The absorbance intensities of the spectra were very similar, as shown in Table 3, with a more noticeable increase in the samples treated at 200 Hz. The bands presented in Table 3 correspond to CH in the CH-O-CH bond (2900 cm⁻¹), NH stretching (1337 cm⁻¹), C-O-H stretching (1150 cm⁻¹), C-O stretching (1102 cm⁻¹), C-C stretching (1078 cm⁻¹), C-O-C stretching (1045, 1022, and 995 cm⁻¹), a glycosidic bond (962 cm⁻¹), and aromatic rings (762 and 703 cm⁻¹). The bands at 1337, 762, and 703 cm⁻¹ indicate the presence of protein and phenolics, which are impurities usually found in starch.

The relative bands corresponding to the C-O stretching vibration in COH groups (region 1150 cm⁻¹) for the plasma-treated samples were slightly more significant than those from the untreated starch samples, indicating that mild modifications were obtained. The bands remained unchanged, indicating that DBD plasma treatment maintains the structural integrity of starch granules [35]. The main changes observed in the molecular structure were related to C-O-H stretching (1150 cm⁻¹), C-O stretching (1102 cm⁻¹), C-C stretching (1078 cm⁻¹), and C-O-C stretching (1045, 1022, and 995 cm⁻¹). The increase in amylopectin

and the changes in the chemical structure indicate that the main reaction is the cross-linking of starch chains initiated by ROS free radicals, probably creating C-O-C bonds between starch or oligosaccharide chains.

The short-range order of starch reflects the order of the double helix and can be measured using FTIR. The attenuated total reflectance (ATR) spectrum is generally used to analyze the short-range ordered structure in the outer region of the starch granule. The range of 1022 cm^{-1} is associated with the amorphous part of the starch. The absorbance at 1045 cm^{-1} is relative to the ordered/crystalline region of the starch. The $1045/1022\text{ cm}^{-1}$ ratio shows the ordered starch grade (ODS), and $995/1022\text{ cm}^{-1}$ reflects the ratio of the amorphous structure to the ordered carbohydrate structure in starch (Table 4). Starch treated at 200 Hz slightly decreased these ratios, indicating a possible change in the ordered structure in the outer region of the starch. The ordered structure in the outer region of the starch has significant effects on the swelling power, sticking viscosity, and hydrolysis because they are linked to the gelatinization stage [36].

Table 4. Short-range ordered structure parameters of corn starch treated using DBD plasma.

Frequency (Hz)	Time (min)	$1045/1022\text{ cm}^{-1}$	$995/1022\text{ cm}^{-1}$
Control	--	0.697	1.279
100	10	0.699	1.263
100	20	0.698	1.275
200	10	0.693	1.294
200	20	0.694	1.273
300	10	0.696	1.277
300	20	0.696	1.277

3.5. Surface Morphology

Figure 2 presents the granular morphology of the starch subjected to plasma. The plasma-treated granules showed a smoother surface than the control sample did. The changes in surface morphology were more evident in the starch treated at 200 Hz than that treated at 100 and 300 Hz. The shape of the granules was maintained, as Gao et al. (2021) [37] reported for plasma-treated sorghum and quinoa starches.

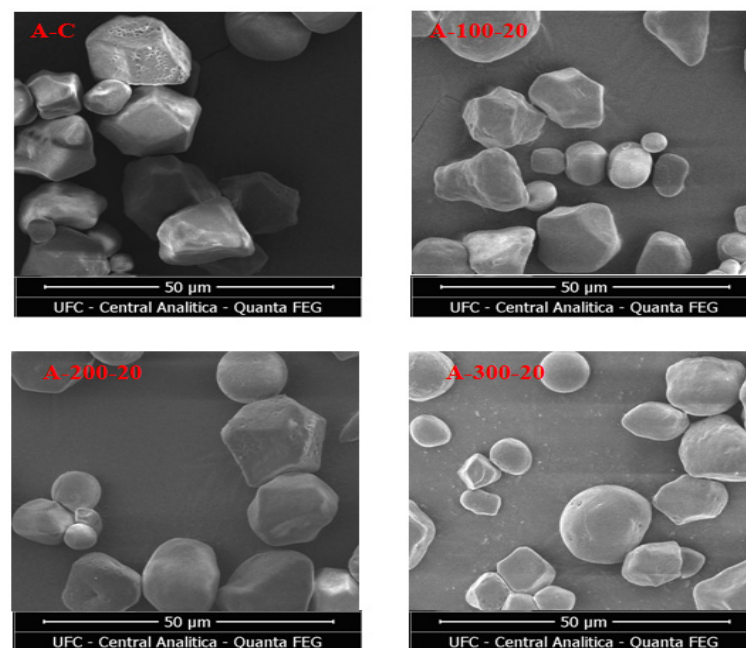


Figure 2. Micrographs of corn starch granules subjected to plasma treatment (magnitude: $2500\times$).

The surface of some starch granules treated at 300 Hz showed cracks and pores due to plasma attack, but its integrity was not affected, as Yan et al. (2020) [33] observed in banana starch. These changes have an essential effect on the molecular and structural properties of the starch molecule. Shen et al. (2022) [38] observed that large pores and a distorted surface of the starch particle allowed reactive plasma species to access the interior of the granule, which resulted in the corrosion and depolymerization of molecules, which was not observed in our SEM images at the three frequencies studied.

The crack and pores observed in the granules treated at 300 Hz did not influence the starch's solubility but may have contributed to the increase in water-holding capacity, as evidenced by the higher water absorption index (Table 2).

3.6. Powder Flowability

Table 5 presents the unconfined yield strength of the untreated and the plasma-treated corn starch. The results presented herein are for corn starch treated for 20 min at 200 Hz because it was the condition that resulted in the most significant changes in corn starch.

Table 5. Unconfined yield strength of untreated and plasma-treated corn starch powder.

Control		Plasma-Treated	
δ_1 (kPa)	δ_c (kPa)	δ_1 (kPa)	δ_c (kPa)
1.212	0.496	1.249	0.571
2.576	0.778	2.555	0.817
4.875	1.019	4.922	1.046
9.158	1.473	10.723	1.031
23.624	2.366	24.785	3.743

The unconfined yield strength (δ_c) indicates the compressive strength of the powder and depends on the stress applied to it (δ_1). This test evidenced that the plasma-treated corn starch had lower flowability since the powder needed greater applied stress to slide.

The flow index of corn starch was 6.75, while the flow index of the plasma-treated corn starch was 6.13. Both powders are classified as easy-flowing powders. This classification is kept the same for plasma treatment despite it having a lower flowability than that of untreated corn starch.

The bulk density and the tapped density of the untreated corn starch were higher than the densities of the plasma-treated starch (Table 6). The compressibility and Hausner indexes were also slightly higher for the untreated corn starch. These properties are related to the shape of the particles, which slightly changed during plasma application, as observed from the SEM micrographs. The higher compressibility index of the untreated starch indicates that plasma treatment resulted in slightly less deformable particles.

Table 6. Density, compressibility, and wall friction angles of untreated and plasma-treated corn starch.

	Untreated	Plasma-Treated
Bulk density (kg/m ³)	421.0	409.1
Tapped density (kg/m ³)	1198.4	1125.1
Compressibility index (%)	43.73	42.99
Hausner ratio	1.78	1.75
Maximum Cohesion (kPa)	0.689	1.112
Minimum wall friction angle (°)	18.6	19.9
Maximum wall friction angle (°)	23.7	26.3

The cohesion represents the interactions between the particle surfaces and ionic and covalent bonding. The plasma-treated corn starch presented higher cohesion which may be related to the chemical changes observed in its structure.

The plasma-treated starch's minimum and maximum wall friction angles were 10% higher than the angles of the untreated starch. Higher wall friction angles indicate a lower

flowability of the starch when it is close to walls. The wall friction angle results corroborate the other flow properties of plasma-treated starch, indicating lower flowability.

4. Conclusions

Cold plasma is an easy-to-operate, efficient, and environmentally friendly physical modification technology that can change starch's molecular characteristics and physicochemical properties. The present study evaluated the effects of DBD technology enhancement on corn starch's physicochemical and structural properties. Treatment at an excitation frequency of 200 Hz for 20 min promoted the most significant variation in amylose content, solubility, and water absorption. These parameters evidenced changes in the starch's physicochemical properties, especially in the amylose to amylopectin ratio, which determines the behavior of many mechanical and barrier properties. The DBD treatment smoothed the surface of the starch granules but caused some cracking on the starch surface when applied at 300 Hz without changing its integrity and structure. The flowability of the plasma-treated corn starch decreased compared to that of the untreated corn starch. However, it has not lost its classification as an easy-flowing powder.

Author Contributions: Investigation, M.L.G.; formal analysis, M.L.G. and F.A.N.F.; writing—original draft, M.L.G.; conceptualization, F.A.N.F.; writing—review and editing, F.A.N.F.; supervision, F.A.N.F. All authors have read and agreed to the published version of the manuscript.

Funding: This work was funded by Coordenação de Aperfeiçoamento de Pessoal de Nível Superior (CAPES) grant Code 001 and Fundação Cearense de Amparo à Pesquisa (FUNCAP) scholarship grant.

Data Availability Statement: Data can be provided upon reasonable request.

Acknowledgments: The authors acknowledge the Central Analítica da Universidade Federal do Ceará for the SEM analysis.

Conflicts of Interest: The authors declare no conflict of interest.

References

1. Wang, X.; Fang, J.; Cheng, L.; Gu, Z.; Hong, Y. Interaction of starch and non-starch polysaccharides in raw potato flour and their effects on thickening stability. *Int. J. Biol. Macromol.* **2023**, *242*, 124702. [[CrossRef](#)]
2. Li, X.; Hu, B.; Ma, R.; Zhang, X.; Sun, C.; Zhao, Y.; Fang, Y. Core-shell starch as a platform for reducing starch digestion and saturated fat intake. *Biomaterials* **2023**, *299*, 122144. [[CrossRef](#)]
3. Sun, X.; Saleh, A.S.; Sun, Z.; Ge, X.; Shen, H.; Zhang, Q.; Yu, X.; Yuan, L.; Li, W. Modification of multi-scale structure, physicochemical properties, and digestibility of rice starch via microwave and cold plasma treatments. *LWT* **2022**, *153*, 112483. [[CrossRef](#)]
4. Apostolidis, E.; Stergiou, A.; Kioupi, D.; Sadeghpour, A.; Paximada, P.; Kakali, G.; Mandala, I. Production of nanoparticles from resistant starch via a simple three-step physical treatment. *Food Hydrocoll.* **2023**, *137*, 108412. [[CrossRef](#)]
5. Luo, W.; Li, B.; Zhang, Y.; Tan, L.; Hu, C.; Huang, C.; Chen, Z.; Huang, L. Unveiling the retrogradation mechanism of a novel high amylose content starch-Pouteria campechiana seed. *Food Chem. X* **2023**, *18*, 100637. [[CrossRef](#)] [[PubMed](#)]
6. Purwitasari, L.; Wulanjati, M.P.; Pranoto, Y.; Witasari, L.D. Characterization of porous starch from edible canna (*Canna edulis* Kerr.) produced by enzymatic hydrolysis using thermostable α -amylase. *Food Chem. Adv.* **2023**, *2*, 100152. [[CrossRef](#)]
7. Luo, X.-E.; Wang, R.-Y.; Wang, J.-H.; Li, Y.; Luo, H.-N.; Zeng, X.-A.; Woo, M.-W.; Han, Z. Combining pulsed electric field and cross-linking to enhance the structural and physicochemical properties of corn porous starch. *Food Chem.* **2023**, *418*, 135971. [[CrossRef](#)] [[PubMed](#)]
8. Liu, M.; Wu, Z.; Meng, Y.; Wang, Z.; He, X.; Gu, J.; Zhang, Y.; Wang, L.; Qin, X. Cationic etherification modification of corn starch and its sizing property. *Text. Res. J.* **2023**, 004051752311638. [[CrossRef](#)]
9. Dong, F.; Gao, W.; Liu, P.; Kang, X.; Yu, B.; Cui, B. Digestibility, structural and physicochemical properties of microcrystalline butyrylated pea starch with different degree of substitution. *Carbohydr. Polym.* **2023**, *314*, 120927. [[CrossRef](#)]
10. Zhu, F. Plasma modification of starch. *Food Chem.* **2017**, *232*, 476–486. [[CrossRef](#)]
11. Jang, H.J.; Jung, E.Y.; Parsons, T.; Tae, H.-S.; Park, C.-S. A Review of Plasma Synthesis Methods for Polymer Films and Nanoparticles under Atmospheric Pressure Conditions. *Polymers* **2021**, *13*, 2267. [[CrossRef](#)] [[PubMed](#)]

12. Guo, Z.; Gou, Q.; Yang, L.; Yu, Q.-L.; Han, L. Dielectric barrier discharge plasma: A green method to change structure of potato starch and improve physicochemical properties of potato starch films. *Food Chem.* **2022**, *370*, 130992. [[CrossRef](#)] [[PubMed](#)]
13. Zou, J.-J.; Liu, C.-J.; Eliasson, B. Modification of starch by glow discharge plasma. *Carbohydr. Polym.* **2004**, *55*, 23–26. [[CrossRef](#)]
14. Goiana, M.L.; de Brito, E.S.; Filho, E.G.A.; Miguel, E.D.C.; Fernandes, F.A.N.; de Azeredo, H.M.C.; Rosa, M.D.F. Corn starch based films treated by dielectric barrier discharge plasma. *Int. J. Biol. Macromol.* **2021**, *183*, 2009–2016. [[CrossRef](#)]
15. Bie, P.; Pu, H.; Zhang, B.; Su, J.; Chen, L.; Li, X. Structural characteristics and rheological properties of plasma-treated starch. *Innov. Food Sci. Emerg. Technol.* **2016**, *34*, 196–204. [[CrossRef](#)]
16. Hernandez-Perez, P.; Flores-Silva, P.C.; Velazquez, G.; Morales-Sanchez, E.; Rodríguez-Fernández, O.; Hernández-Hernández, E.; Mendez-Montealvo, G.; Sifuentes-Nieves, I. Rheological performance of film-forming solutions made from plasma-modified starches with different amylose/amylopectin content. *Carbohydr. Polym.* **2020**, *255*, 117349. [[CrossRef](#)] [[PubMed](#)]
17. Okyere, A.Y.; Boakye, P.G.; Bertoft, E.; Annor, G.A. Temperature of plasma-activated water and its effect on the thermal and chemical surface properties of cereal and tuber starches. *Curr. Res. Food Sci.* **2022**, *5*, 1668–1675. [[CrossRef](#)]
18. Lii, C.Y.; Liao, C.D.; Stobinski, L.; Tomasik, P. Behaviour of granular starches in low-pressure glow plasma. *Carbohydr. Polym.* **2002**, *49*, 499–507. [[CrossRef](#)]
19. Carvalho, A.P.M.G.; Barros, D.R.; da Silva, L.S.; Sanches, E.A.; Pinto, C.D.C.; de Souza, S.M.; Clerici, M.T.P.S.; Rodrigues, S.; Fernandes, F.A.N.; Campelo, P.H. Dielectric barrier atmospheric cold plasma applied to the modification of Ariá (*Goeppertia allouia*) starch: Effect of plasma generation voltage. *Int. J. Biol. Macromol.* **2021**, *182*, 1618–1627. [[CrossRef](#)]
20. Shen, H.; Ge, X.; Zhang, Q.; Zhang, X.; Lu, Y.; Jiang, H.; Zhang, G.; Li, W. Dielectric barrier discharge plasma improved the fine structure, physicochemical properties and digestibility of α -amylase enzymatic wheat starch. *Innov. Food Sci. Emerg. Technol.* **2022**, *78*, 102991. [[CrossRef](#)]
21. Chaiwat, W.; Wongsagonsup, R.; Tangpanichyanon, N.; Jariyaporn, T.; Deeyai, P.; Suphantharika, M.; Fuongfuchat, A.; Nisoa, M.; Dangtip, S. Argon Plasma Treatment of Tapioca Starch Using a Semi-continuous Downer Reactor. *Food Bioprocess Technol.* **2016**, *9*, 1125–1134. [[CrossRef](#)]
22. Fernandes, F.A.; Santos, V.O.; Rodrigues, S. Effects of glow plasma technology on some bioactive compounds of acerola juice. *Food Res. Int.* **2018**, *115*, 16–22. [[CrossRef](#)] [[PubMed](#)]
23. Marenco-Orozco, G.A.; Rosa, M.F.; Fernandes, F.A.N. Effects of multiple-step cold plasma processing on banana (*Musa sapientum*) starch-based films. *Packag. Technol. Sci.* **2022**, *35*, 589–601. [[CrossRef](#)]
24. Hu, J.; Cheng, F.; Lin, Y.; Zhao, K.; Zhu, P. Dissolution of starch in urea/NaOH aqueous solutions. *J. Appl. Polym. Sci.* **2016**, *133*, 43390. [[CrossRef](#)]
25. Fang, C.; Huang, J.; Pu, H.; Yang, Q.; Chen, Z.; Zhu, Z. Cold-water solubility, oil-adsorption and enzymolysis properties of amorphous granular starches. *Food Hydrocoll.* **2021**, *117*, 106669. [[CrossRef](#)]
26. Chen, G.; Chen, Y.; Jin, N.; Li, J.; Dong, S.; Li, S.; Zhang, Z. Zein films with porous polylactic acid coatings via cold plasma pre-treatment. *Ind. Crop. Prod.* **2020**, *150*, 112382. [[CrossRef](#)]
27. Warren, F.J.; Gidley, M.J.; Flanagan, B.M. Infrared spectroscopy as a tool to characterise starch ordered structure—A joint FTIR-ATR, NMR, XRD and DSC study. *Carbohydr. Polym.* **2016**, *139*, 35–42. [[CrossRef](#)]
28. Lima, A.C.d.S.; Afonso, M.R.A.; Rodrigues, S.; de Aquino, A.C. Flowability of spray-dried saponin powder. *J. Food Process. Eng.* **2022**, *45*, e14092. [[CrossRef](#)]
29. Filho, E.G.A.; Cullen, P.J.; Frias, J.M.; Bourke, P.; Tiwari, B.K.; Brito, E.S.; Rodrigues, S.; Fernandes, F.A. Evaluation of plasma, high-pressure and ultrasound processing on the stability of fructooligosaccharides. *Int. J. Food Sci. Technol.* **2016**, *51*, 2034–2040. [[CrossRef](#)]
30. Almeida, F.D.L.; Gomes, W.F.; Cavalcante, R.S.; Tiwari, B.K.; Cullen, P.J.; Frias, J.M.; Bourke, P.; Fernandes, F.A.; Rodrigues, S. Fructooligosaccharides integrity after atmospheric cold plasma and high-pressure processing of a functional orange juice. *Food Res. Int.* **2017**, *102*, 282–290. [[CrossRef](#)]
31. DeNardin, C.C.; da Silva, L.P. Estrutura dos grânulos de amido e sua relação com propriedades físico-químicas. *Ciência Rural* **2009**, *39*, 945–954. [[CrossRef](#)]
32. Thirumdas, R.; Trimukhe, A.; Deshmukh, R.; Annapure, U. Functional and rheological properties of cold plasma treated rice starch. *Carbohydr. Polym.* **2017**, *157*, 1723–1731. [[CrossRef](#)]
33. Yan, S.; Chen, G.; Hou, Y.; Chen, Y. Improved solubility of banana starch by dielectric barrier discharge plasma treatment. *Int. J. Food Sci. Technol.* **2020**, *55*, 641–648. [[CrossRef](#)]
34. Kizil, R.; Irudayaraj, J.; Seetharaman, K. Characterization of Irradiated Starches by Using FT-Raman and FTIR Spectroscopy. *J. Agric. Food Chem.* **2002**, *50*, 3912–3918. [[CrossRef](#)] [[PubMed](#)]
35. Ge, X.; Guo, Y.; Zhao, J.; Zhao, J.; Shen, H.; Yan, W. Dielectric barrier discharge cold plasma combined with cross-linking: An innovative way to modify the multi-scale structure and physicochemical properties of corn starch. *Int. J. Biol. Macromol.* **2022**, *215*, 465–476. [[CrossRef](#)]
36. Wang, J.; Guo, K.; Fan, X.; Feng, G.; Wei, C. Physicochemical Properties of C-Type Starch from Root Tuber of *Apios fortunei* in Comparison with Maize, Potato, and Pea Starches. *Molecules* **2018**, *23*, 2132. [[CrossRef](#)]

37. Gao, S.; Liu, H.; Sun, L.; Cao, J.; Yang, J.; Lu, M.; Wang, M. Rheological, thermal and in vitro digestibility properties on complex of plasma modified Tartary buckwheat starches with quercetin. *Food Hydrocoll.* **2020**, *110*, 106209. [[CrossRef](#)]
38. Shen, H.; Ge, X.; Zhang, B.; Su, C.; Zhang, Q.; Jiang, H.; Zhang, G.; Yuan, L.; Yu, X.; Li, W. Preparing potato starch nanocrystals assisted by dielectric barrier discharge plasma and its multiscale structure, physicochemical and rheological properties. *Food Chem.* **2022**, *372*, 131240. [[CrossRef](#)]

Disclaimer/Publisher's Note: The statements, opinions and data contained in all publications are solely those of the individual author(s) and contributor(s) and not of MDPI and/or the editor(s). MDPI and/or the editor(s) disclaim responsibility for any injury to people or property resulting from any ideas, methods, instructions or products referred to in the content.